JOURNAL OF SOLID STATE CHEMISTRY 105, 263–270 (1993)

Composition- and Annealing-Dependent Properties of $Ba(Bi,Tl)O_{3-\delta}$

THOMAS E. SUTTO AND BRUCE A. AVERILL*

Chemistry Department, University of Virginia, Charlottesville, Virginia 22901

Received July 20, 1992; in revised form November 16, 1992; accepted November 17, 1992

Solid solutions of $BaBiO_3$ doped with thallium to give $BaBi_{1-x}Tl_xO_{3-\delta}$ were prepared at 800°C and annealed at 425°C under either argon, air, or oxygen. All samples with $x \leq 0.4$ showed an increase in the semiconducting band gap that was accompanied by a decrease in the room temperature diamagnetism, regardless of annealing conditions. Samples with $x \leq 0.4$ also exhibited orthorhombic symmetry, rather than monoclinic, as for the parent $BaBiO_3$. For compositions centered around $BaBi_{0.5}Tl_{0.5}O_{3-\delta}$, however, the resistivity, susceptibility, and structural data were dependent upon the annealing conditions. Insulating behavior and strong diamagnetism (-6.15×10^{-7} emu/g) were observed for the argon-annealed sample, which had $\delta = 0.84$ and possessed tetragonal symmetry with $a = 6.0724$ and $c = 8.9101$ Å. The air-annealed sample had a value of $\delta = 0.46$, was a semiconductor or semimetal with a transition to metallic behavior at 73 K, and exhibited moderate room temperature diamagnetism (-3.17×10^{-7} emu/g) and an orthorhombic unit cell with $a = 6.0713$, $b = 6.1123$, and $c = 8.5790$ Å. Oxygen annealing gave a material with $\delta = 0.0$ that was weakly semiconducting and weakly diamagnetic at room temperature (-0.35×10^{-7} emu/g), and possessed a tetragonal unit cell with $a = 6.0778$ and $c = 8.5418$ Å. These results are interpreted in terms of the extent and possible ordering of the oxygen vacancies and/or metal atoms.

Because it is the parent compound for three metal oxide superconductors (Ba(Bi,Pb)O_3, peak T_c 13.5 K (*1*); (Ba,K)BiO_3, peak T_c 32 K (*2*); and Ba(Bi,Pb,Tl)O_3, peak T_c 10.5 K (*3*), $BaBiO_3$ has been extensively studied. Like La_2CuO_4, $BaBiO_3$ is a complex metal oxide perovskite that exhibits semiconducting behavior rather than the metallic conductivity predicted by band structure calculations (*4,5*).

The failure of classic band structure theory to accurately predict the semiconductive nature of $BaBiO_3$ is due to the disproportionation of the Bi sites. Band structure calculations were performed on the assumption that the valence of Bi is close to 4+ (*4*). However, single crystal X-ray diffraction (*6*) and neutron diffraction (*7*) studies indicate that the Bi atoms are located on two distinct crystallographic sites with different Bi–O bond lengths. For one site, the Bi–O bond lengths are near those observed for Bi^{5+}, while the other site possesses Bi–O bond lengths slightly shorter than those normally observed for Bi^{3+}, indicating a high degree of overlap between Bi and O. These data suggest that the material is not in fact $BaBi^{4+}O_3$, but is instead more properly formulated as $Ba_2Bi^{3+}Bi^{5+}O_6$. This disproportionation is believed to result in a charge density wave- (CDW-) induced gap at the Fermi surface (E_f) in the parent compound, causing the observed semiconducting behavior.

In contrast to $BaBiO_3$, $BaPbO_3$ obeys band structure calculations. It possesses a nearly ideal cubic structure, with a slight (ca. 9°) rotation of the oxygen octahedra around each Pb site. The material exhibits metallic conduction down to 0.5 K, where it is reported to undergo a superconducting transition (*8*). Metallic conduction in this system is attributed to delocalization of the O 2*p* electrons into the empty 6*s* band of Pb^{4+}.

* To whom correspondence should be addressed.

0022-4596/93 $5.00

In both the $Ba(Bi,Pb)O_3$ and $(Ba,K)BiO_3$ systems, the onset of superconducting behavior has been related to a decrease in the magnitude of the CDW-induced semiconducting gap of $BaBiO_3$ (*9*), since CDW and superconductivity are competing states (*10*). In the case of the $Ba(Bi,Pb)O_3$ system, band structure calculations indicate that the gap induced at E_f by the CDW is considerably diminished at the point where metallic behavior gives way to superconductivity (*11*). $(Ba,K)BiO_3$ is also reported to give rise to a reduction in the CDW-induced gap.

The most recent development in the chemistry of the $BaMO_3$ system (where M is one of the three 6*s* valence metals Tl, Bi, or Pb) is the discovery of $Ba_4BiPb_2TlO_{12-\delta}$ (*3*). As described elsewhere, the properties of this system are extremely sensitive to changes in the composition, and deviation by more than 5% from the ideal Bi, Tl, or Pb composition results in a loss of superconducting behavior (*12*). The unique aspect of this material as opposed to the Ba–K–Bi–O and the Ba–Bi–Pb–O systems is that the presence of oxygen vacancies appears to be required for superconductivity. In the parent $Ba_4BiPb_2TlO_{12}$ compound without oxygen vacancies, the metals all possess a $6s^0$ configuration. The presence of oxygen vacancies results in reduction of the metals, repopulation of the 6*s* band, and superconductivity (*3,12*).

In the present work, solid solutions of $BaBiO_3$ doped with Tl were examined as a way of increasing the oxidation state of Bi and decreasing the population of the 6*s* band. Recent Mössbauer studies of Sb-doped $BaBiO_3$ indicate that only Sb^{5+} can substitute into $BaBiO_3$ without significantly altering its conductive and structural properties (*13*). This indicates that a unique Bi^{5+} site exists and can be preferentially substituted. On the basis of charge and size considerations, one might therefore expect that Tl^{3+} ($6s^0$) should substitute preferentially into the Bi^{3+} ($6s^2$) sites. In the absence of oxygen vacancies, this should result in an increase in the semiconducting gap due to the lowering of E_f and lead to a decrease in the high temperature diamagnetism observed in $BaBiO_3$ due to a reduction of the number of $6s^2$ electron pairs (*14*). This should also alleviate the monoclinic distortion of $BaBiO_3$, which is attributed to the presence of $6s^2$ electron pairs that produce a pseudo-Jahn–Teller distortion (*15*). The present work demonstrates that the extent and possibly the ordering of oxygen vacancies and/or Tl atoms in $Ba(Bi,Tl)O_3$ result in a remarkable range of observed properties.

Experimental

Synthesis. Solid solutions of $BaBi_{1-x}Tl_xO_3$ ($x = 0.0, 0.1, 0.2, 0.3, 0.4, 0.5, 0.6$, and 0.7) were prepared in sintered Al_2O_3 boats with 99.999% Bi_2O_3, 99% Tl_2O_3, and 99.999% $BaCO_3$ (Aldrich). Stoichiometric amounts of Bi_2O_3 and $BaCO_3$ and a 15% excess of Tl_2O_3 were ground for 4 min in a wiggle bug. Three pellets were pressed from each of the powder mixtures and loaded into sintered Al_2O_3 boats. The samples were then placed in a quartz tube and heated for 2 hr at 800°C under flowing air (5–10 cm^3/min). Samples were allowed to cool to room temperature in the oven, divided into three complete sets of pellets, heated to 425°C (4°C/min), and then reannealed under either argon, air, or O_2 for 1.5 hr with a flow rate of 5–10 cm^3/min. Pellets were then cooled (20°C/hr) to room temperature in the oven under the appropriate gas flow.

Methods. X-ray data were obtained on a Scintag powder diffractometer with a scan rate of 2°/min over a 2Θ range of 5–75° in 0.01° steps. The resulting powder patterns were indexed and analyzed by a Fortran IV X-ray fitting program (*16*). Average peak width at half-height was 1.1° for the 101, 002, and 102 lines.

Resistivity data were measured on a four-probe resistivity system using a Lake Shore temperature sensor with a calibrated Si diode (±0.05 K) and a 20-mA (±0.02 mA) constant current source. Resulting voltages

were measured with a Kiethley voltmeter with a sensitivity of 0.5 μV.

Susceptibility data were obtained on a S.H.E. magnetic susceptometer operating at 20 G to detect superconducting transitions and at 25 kG for bulk magnetic susceptibility from 50 to 300 K. The value of the Pauli diamagnetism was determined by the linear portion of the magnetic data between the temperatures of 50 and 200 K.

Flame atomic emission (FAE) data were measured on a Perkin-Elmer 510 atomic absorption instrument, equipped with an acetylene/nitrous oxide gas mixture. All samples were weighed in triplicate prior to dissolving them in aqua regia. Analytical data are reported based on a content of 1.0 Ba per formula unit. For all values of x, FAE indicated that the observed Tl content was within $\pm 0.07\%$ of the expected value. Oxygen contents were determined by difference using the measured Ba, Tl, Bi, and Pb percentages; estimated errors are $\pm 0.26\%$ or $\Delta\delta = \pm 0.13$. Because of the volatility of Tl_2O and secondary chemical interferences, direct determination of the oxygen content by previously published techniques is not feasible.

Discussion

Observation of the pellets indicate that the orange-gold color of the undoped material changed to a dark brown-black color for the $x = 0.40$ material, regardless of the annealing conditions. For the $x = 0.50$ sample, both the oxygen and air-annealed samples were black, while the argon-annealed sample was a gray-black color. Elemental analysis data are reported in Table I. The dependence of the extent of oxygen vacancies on composition and annealing conditions in $BaBi_{1-x}Tl_xO_{3-\delta}$ is shown in Fig. 1.

X-ray diffraction analysis indicated the presence of a single phase up to $x = 0.5$ under all annealing conditions, with no excess Tl_2O_3 remaining. For higher values of x, diffraction lines corresponding to $Ba_2Tl_2O_5$ as well as secondary perovskite phases were observed. As shown in Fig. 2, orthorhombic symmetry was observed for samples with $x = 0.2$, and further doping with thallium led to a decrease in the orthorhombic symmetry until a tetragonal unit cell was observed for the $x = 0.50$ material. For all samples except those with $x = 0.50$, no structural differences were observed between the argon-, air-, and oxygen-annealed samples, and all lattice parameters fell within experimental error for each value of x.

The structure of the $x = 0.50$ material, however, depended dramatically upon the annealing atmosphere. Argon annealing of the 50% doped material gave rise to a material with a tetragonal unit cell ($a = 6.0724$ and $c = 8.9101$ Å). Oxygen annealing also resulted in tetragonal symmetry, but with $a = 6.0778$ and $c = 8.5418$ Å. However, air annealing gave rise to a material with an orthorhombic unit cell ($a = 6.0713$, $b = 6.1123$, and $c = 8.5790$ Å).

The presence of a tetragonal unit cell for the oxygen-annealed $x = 0.5$ sample (with $\delta \sim 0.0$) and the gradual conversion to tetragonal unit symmetry with increasing x are expected due to the loss of the pseudo-Jahn–Teller distorting $6s^2$ electron pairs. However, the change to an orthorhombic unit cell for the air-annealed sample (with $\delta \sim 0.5$) indicates that a structural transition is induced by the loss of nearly half an oxygen atom per unit cell. Analogous structural changes due to oxygen vacancies have been observed in $BaBiO_{3-y}$ (*17*), where stable new forms of the parent material have been found to exist for $y = 0.03$ and 0.23, which are monoclinic and cubic, respectively. The unusual point about air-annealed $BaBi_{0.5}Tl_{0.5}O_{(3-\delta)}$ is the large extent of oxygen vacancies, approximately twice that found to be stable in $BaBiO_3$. The most likely explanation is that partial reduction of Tl is occurring. Since Tl^{1+} is 0.52 Å larger than Bi^{3+} and 0.73 Å larger than Bi^{+5} (*18*), the increased size of Tl compared to Bi might well be enough to lead to ordering of the metal sites (*19*).

TABLE I

ANALYTICAL DATA FOR $BaBi_{1-x}Tl_xO_{3-\delta}$ ANNEALED UNDER ARGON, AIR, OR OXYGEN

Annealing condition	Nominal x	Tl stoichiometry (x)	Bi stoichiometry	δ
Argon	*0.00*	*0.00(0)*	*0.99(7)*	0.03
	0.10	0.09(8)	0.90(0)	0.01
	0.20	0.20(2)	0.79(4)	0.11
	0.30	0.29(6)	0.70(2)	0.08
	0.40	0.39(9)	0.59(6)	0.27
	0.50	0.49(8)	0.49(8)	0.81
Air	*0.00*	*0.00(0)*	*0.99(9)*	0.01
	0.10	0.09(8)	0.92(3)	0.01
	0.20	0.20(3)	0.79(7)	0.02
	0.30	0.29(8)	0.69(9)	0.08
	0.40	0.39(8)	0.61(1)	0.13
	0.50	0.49(7)	0.49(8)	0.46
Oxygen	*0.00*	*0.000*	*1.00(1)*	−0.01
	0.10	0.09(2)	0.92(3)	−0.05
	0.20	0.20(0)	0.80(3)	0.00
	0.30	0.30(2)	0.69(8)	0.02
	0.40	0.39(9)	0.58(9)	−0.01
	0.50	0.50(2)	0.50(4)	−0.02

Reduction of the metals, which results in a repopulation of the 6*s* levels, might be expected to cause a pseudo-Jahn–Teller distortion, with a further decrease in symmetry for the argon-annealed $x = 0.50$ sample. A tetragonal unit cell with an elongated *c*-axis is observed, which is characteristic of a two-dimensional system subject to a Jahn–Teller induced distortion (*20*). Unfortunately, the available structural data cannot distinguish between a two-dimensional or three-dimensional structure due to the similar electron densities of Tl and Bi.

Below 100 K the resistivity of the samples was too high to be measured accurately, but

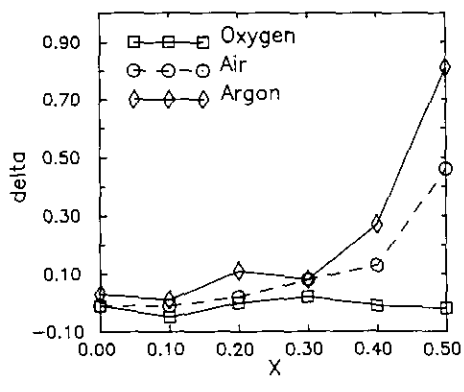

FIG. 1. Plot of δ for $BaBi_{1-x}Tl_xO_{3-\delta}$ annealed in oxygen, air, or argon.

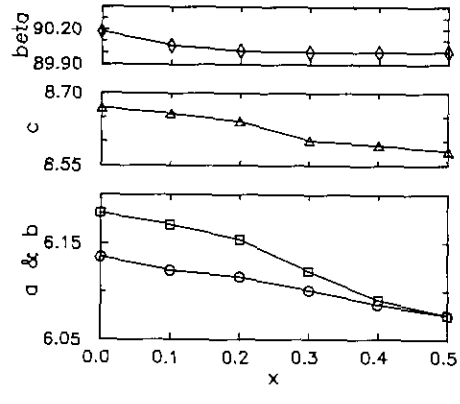

FIG. 2. Plot of a, b, and c in Å and β in ° vs x for oxygen-annealed $BaBi_{1-x}Tl_xO_{3-\delta}$.

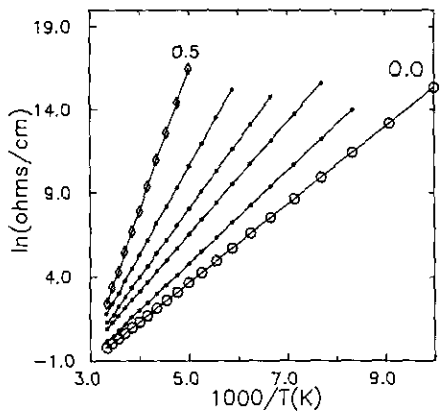

FIG. 3. Log plot of resistivity vs inverse temperature for samples of oxygen-annealed $BaBi_{1-x}Tl_xO_{3-\delta}$ with $x = 0.0$–0.5.

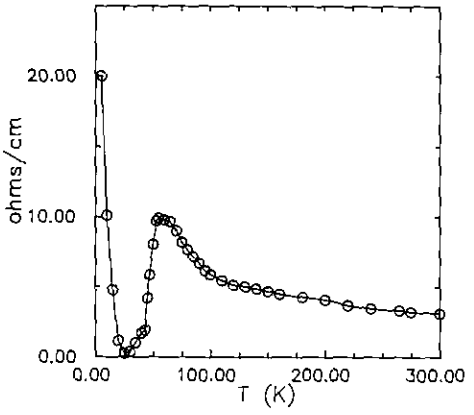

FIG. 5. Plot of resistivity vs temperature for air-annealed $BaBi_{0.5}Tl_{0.5}O_{3-\delta}$.

measurements were continued down to 4 K to ensure that no unusual electronic transition occurred. As shown in Fig. 3 for the oxygen-annealed materials, the nesting of the log plots of the resistivity vs the inverse temperature over the range 100 K $\leq T \leq$ 298 K for $x \leq 0.40$ indicates a widening of the semiconducting gap as Tl is substituted for Bi. The air- and argon-annealed samples with $x \leq 0.4$ exhibited similar behavior. Figure 4 illustrates the changes in the band gap calculated from the slope of the log plot of the resistivity. The increase in the band gap for all samples up to $x \leq 0.4$ provides evidence that Tl doping is depopulating the 6*s* band, lowering E_f, and thus increasing the observed semiconducting gap.

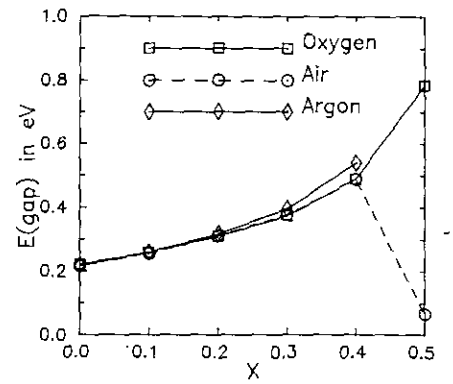

FIG. 4. Plot of semiconducting band gap, E_{gap}, vs x for $BaBi_{1-x}Tl_xO_{3-\delta}$ annealed under oxygen, air, or argon.

However, the electronic properties of $BaBi_{0.5}Tl_{0.5}O_{3-\delta}$ are strongly dependent upon the oxygen content, as shown in Fig. 4. The argon-annealed sample was insulating, with a room temperature resistivity of over 40 kΩ/cm, and is therefore excluded from Fig. 4. However, the air-annealed $x = 0.5$ material showed very strong semiconducting, or possibly semimetallic, behavior down to 73 K, where it underwent a semiconductor to metal transition (Fig. 5), followed by a secondary transition into a poorly semiconducting or insulating state at 20 K. This behavior is attributed to the presence of a high degree of oxygen vacancies in the argon-annealed sample ($\delta = 0.84$), resulting in a loss of the delocalized O 2*p* band and insulating behavior. The properties of the oxygen-annealed sample, with $\delta = 0.0$, indicate that without oxygen vacancies the material behaves as predicted for a system with a depopulated 6*s* band. However, the metallic conductivity of the air-annealed sample, with $\delta = 0.46$, indicates that the presence of partial oxygen vacancies results in repopulation of the 6*s* band. The conductive anomalies could be explained as arising from either ordered oxygen vacancies or metal centers leading to a change in the overall dimensionality of the system. The

sudden increase in the resistance at low temperature is characteristic of the trapping of conduction electrons in the oxygen vacancies, resulting in insulating behavior (*21*).

As shown in Fig. 6, the doping of Tl into $BaBiO_3$ induced a gradual decrease in the strength of the diamagnetic signal for $0.1 \leq x \leq 0.40$. As the temperature was decreased, a gradual decrease in the magnitude of diamagnetic signal was observed for both the argon- and air-annealed samples, probably due to the presence of small amounts of paramagnetic impurities. However, significant differences were observed for the 50% doped samples depending upon annealing conditions.

At room temperature, the oxygen-annealed sample showed a very weak diamagnetic signal of -3.67×10^{-8} emu/g, while the argon-annealed sample gave rise to a much stronger diamagnetic signal of -6.11×10^{-7} emu/g. The most dramatic effects were observed for the air-annealed sample. As shown in Fig. 7, this sample changed from diamagnetic ($\chi = 3.14 \times 10^{-7}$ emu/g) at room temperature to a temperature-independent paramagnetism of ca. 10^{-6} emu/g from 73 to 20 K; below 20 K, a sudden increase in paramagnetic signal was observed. This indicates that the anomalous conductivity observed for the system is accompanied by magnetic transitions. The transition from diamagnetism to paramagnetism at 120 K, followed by the nearly linear portion of the susceptibility curve over the region for which the sample exhibits metallic conduction, indicates that a significant population of the conduction band by unpaired electrons at E_f is occurring. The trapping of electron pairs in the material would significantly depopulate this conduction band, leading to weak paramagnetism as observed (*21*).

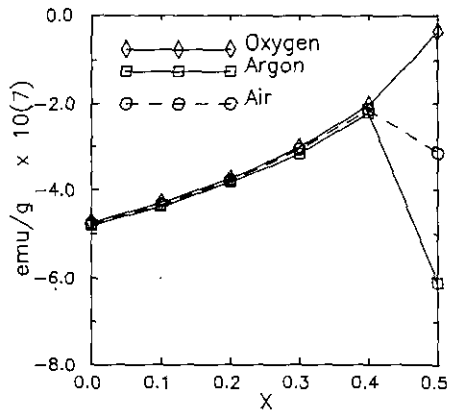

FIG. 6. Plot of diamagnetic susceptibility in emu/g vs x for $BaBi_{1-x}Tl_xO_{3-\delta}$ annealed under oxygen, air, and argon.

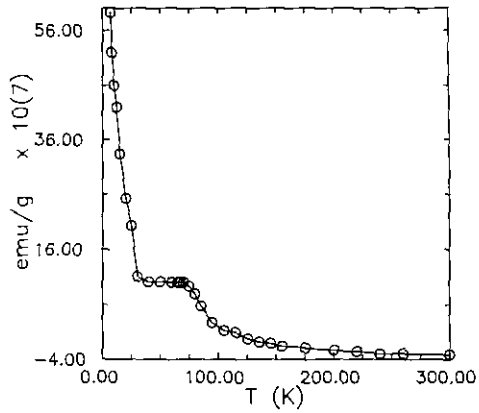

FIG. 7. Plot of susceptibility in emu/g vs T in K for air-annealed $BaBi_{0.5}Tl_{0.5}O_{3-\delta}$.

Previous studies of Tl-doped $BaBiO_3$ by Subramanian *et al.* (*22*), Wang *et al.* (*23*), and Li *et al.* (*24*) found significantly different solubilities and physical properties. Sleight reports a pseudocubic unit cell and solubility for Tl up to $x = 0.8$ (*22*). It was also reported that the resistivity decreasing with increasing x, leading to semimetallic behavior in $BaBi_{0.4}Tl_{0.6}O_3$. In contrast, Wang *et al.* (*23*) reported that Tl doping led to an orthorhombic unit cell, with a solubility limit of only 30% Tl; a monotonic increase in resistivity was observed upon Tl doping. Li *et al.* (*24*) reported the existence of a monoclinic phase below $x = 0.2$ and an orthorhombic phase for $0.40 < x \leq 0.50$, with a mixed phase region occurring at $0.20 < x < 0.40$; the orthorhombic phase exhibited a resistivity two orders of magnitude lower than the monoclinic phase. No magnetic

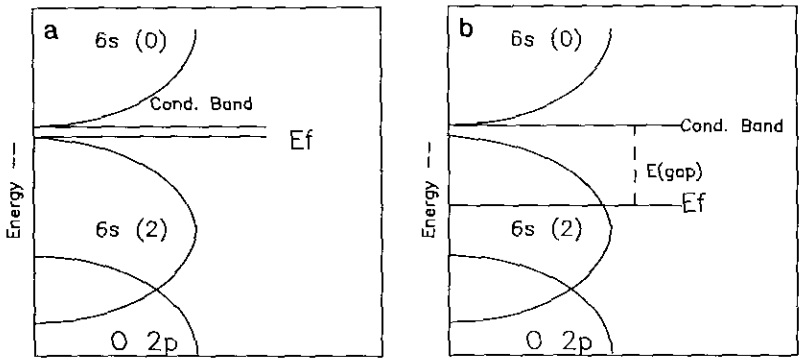

FIG. 8. Schematic band structure for (a) $BaBiO_3$, (b) $BaBi_{1-x}Tl_xO_3$ ($x \leq 0.40$).

data have been reported previously. The apparent discrepancies in the reported properties are difficult to interpret due to the lack of chemical analysis data on the previous preparations and the different methods used to prepare the materials. Subramanian *et al.* prepared samples at 850°C in sealed gold tubes (*22*), a procedure which might result in the formation of samples with sufficient oxygen deficiencies to accommodate the higher Tl content. Wang *et al.* synthesized samples at 725°C under nitrogen (*23*), followed by heating at 450°C under oxygen, while Li *et al.* heated samples for 24 hr at 750°C (*24*); both of these procedures could have led to a significant loss of Tl. As a result of these differences, detailed comparisons between the previous studies of $Ba(Bi,Tl)O_3$ and the work presented here are not possible.

The failure of the band structure calculated for $BaBi^{+4}O_3$ to accurately predict the conductive nature of the material, the recent discovery in ellipsometry measurements of $BaBiO_3$ (*25*) of unexplainable transitions near E_f, and the observed doping properties of 3+ and 5+ metal ions into the Bi sites clearly indicate that the properties of $BaBiO_3$ cannot be explained by any band structure based upon a Bi valence near 4+. Instead, the best explanation of the observed physical changes upon Tl doping is that Bi in $BaBiO_3$ is disproportionated into two sites, one of which approximates Bi^{3+}, possessing strongly localized $6s^2$ electron pairs and an empty conduction band formed by the overlap of the O $2p$ band, and the non-Jahn–Teller distorted Bi^{5+} metal sites as shown in Fig. 8a. Tl doping, therefore, depopulates the $6s^2$ electron pairs at the localized sites, leading to an increase in the observed semiconducting band gap (Fig. 8b).

Conclusion

The observed structural and resistivity patterns of $BaBi_{(1-x)}Tl_xO_{(3-\delta)}$ for $x \leq 0.4$ clearly indicate the presence of a 3+ metal center that can be substituted without altering the general structure or conductive properties of the parent material. The annealing-dependent structural and resistivity properties of $BaBi_{0.5}Tl_{0.5}O_{3-\delta}$ are attributed to changes in the oxygen content accompanied by ordering of the oxygen vacancies and/or metal sites.

References

1. A. W. SLEIGHT, J. L. GILLSON, AND P. E. BIERSTEDT, *Solid State Commun.* **17**, 27 (1975).
2. L. F. MATTHEISS, E. M. GYORGY, AND D. W. JOHNSON, JR., *Phys. Rev. B* **37**, 3745 (1988).
3. T. E. SUTTO, B. A. AVERILL, AND J. RUVALDS, *Chem. of Mater.* **3**, 209 (1991).
4. L. F. MATTHIESS AND D. R. HAMANN, *Phys. Rev. B* **28**, 4227 (1983).
5. L. F. MATTHEISS, *Phys. Rev. Lett* **58**, 1028 (1987).
6. D. E. COX AND A. W. SLEIGHT, *Acta Crystallogr Sect. B* **35**, 1 (1979).

7. C. Chaillout and A. Santoro, *Solid State. Commun.* **65,** 1363 (1988).
8. A. W. Sleight, *in* "High Temperature Superconducting Materials" (W. E. Hatfield and J. Miller, Eds.) p. 6, Wiley, New York (1988).
9. S. Pei, N. J. Zaluzec, J. D. Jorgensen, B. Dabrowski, D. G. Hinks, A. W. Mitchell, and D. R. Richards, *Phys. Rev. B* **44,** 9547 (1991).
10. Z.-X. Shen, P. A. P. Lindberg, B. O. Wells, D. S. Dessau, A. Borg, I. Lindau, W. E. Spicer, W. P. Ellis, G. H. Kwei, K. C. Oh, J. S. Kang, and J. W. Allen, *Phys. Rev. B* **40,** 6912 (1989).
11. S. Tajima, S. Uchida, A. Masaki, H. Takagi, K. Kitazawa, S. Tanaka, and S. Sugai, *Phys. Rev. B* **35,** 696 (1987).
12. T. E. Sutto and B. A. Averill, *Chem. of Mater.*, **4,** 1092 (1992).
13. M. Eibshutz, R. J. Cava, J. J. Kajewski, and W. F. Peck, Jr., *Appl. Phys. Lett.* **58,** 1914 (1991).
14. C. A. Balseiro and L. M. Falicov, *in* "Superconductivity in *d*- and *f*- Band Metals" (H. Suhl and M. B. Maple, Eds.), p. 105, Academic Press, New York (1980).
15. A. F. Wells, *in* "Structural Inorganic Chemistry", 5th ed. p. 1074, Oxford Univ. Press, Oxfordshire (1984).
16. C. W. Clark, D. K. Smith, and G. Johnson, Fortran IV X-Ray Powder Diffraction Program (1973).
17. G. Le Flem, G. Demazeau, and P. Hagenmuller, *J. Solid State Chem.* **44,** 82 (1982).
18. Table of Ionic Radii, *in* "CRC Handbook of Chemistry and Physics" (R. Weast, Ed.), 70th Edition, p. F-214 (1991).
19. A. F. Wells, *in* "Structural Inorganic Chemistry," 5th ed. p. 588, Oxford Univ. Press, Oxfordshire (1984).
20. A. F. Wells, *in* "Structural Inorganic Chemistry", 5th ed., p. 584 Oxford Univ. Press, Oxfordshire (1984).
21. F. J. Di Salvo, J. A. Wilson, B. G. Bagley, and J. Waszczak, *Phys. Rev. B* **12,** 2220 (1975).
22. R. Subramanian, M. Subramanian, and A. W. Sleight, *Bull. Mater. Sci.*, **24,** 1413 (1989).
23. E. Wang, J.-M. Tarascon and G. W. Hull, *Solid State Commun.* **74,** 471 (1990).
24. S. Li, K. V. Ramanujachary, and M. Greenblatt, *Physica C* **166,** 535 (1990).
25. Y.-Y. Wang, G. F. Feng, T. E. Sutto, and Z. Shao, *Phys. Rev. B* **44,** 7098 (1991).